myjournal manuscript No.
(will be inserted by the editor)

Free charge carrier absorption in silicon at 800 nm

P.-C. Heisel[1⋆], W. I. Ndebeka[2], P. H. Neethling[2], W. Paa[1], E. G. Rohwer[2], C. M. Steenkamp[2], H. Stafast[1,2]

[1] Leibniz Institute of Photonic Technology, Albert-Einstein-Str. 9, 07745 Jena, Germany
[2] Laser Research Institute, Department of Physics, University of Stellenbosch, P. Bag X1, Matieland 7602, South Africa

Received: date / Revised version: date

Abstract The transmission of a Ti:sapphire laser beam (c.w. and fs pulsed operation at 800 nm) through a 10 µm thin oxidized silicon membrane at 45° angle of incidence at first increases with the incident laser power, then shows a maximum, and finally decreases considerably. This nonlinear transmission behavior is the same for c. w. and pulsed laser operation and mainly attributed to free charge carrier (FCA) absorption in Si. A simple FCA model is developed and tested.

1 Introduction

Today silicon (Si) continues to be a prominent material in microelectronics, optoelectronics, micromechanics, solar cells, and increasingly in photonics. To prepare, modify and/or shape Si material and delicate Si devices, a broad spectrum of techniques has been established. In particular laser technology provides a manifold of remote, contactless, spatially confined and time controlled methods for e.g. doping, annealing, crystallization, and ablation. These require, however, a proper control and understanding of the linear and nonlinear optical properties of Si. Typically laser light shows a narrow spectral bandwidth, high intensity as well as spatial and temporal confinement. Therefore particularly the nonlinear optical properties of Si are of utmost importance including their laser induced changes by heating and/or electronic excitation.

Some of the nonlinear optical properties of Si may occur simultaneously and be difficult to discriminate like e.g. coherent two-photon absorption (TPA), free carrier absorption (FCA), and thermally induced absorption enhancement (TAE) [1]. Moison et al. argue that TAE is dominant over FCA for probe photon energies $h\nu \geq 2\,\mathrm{eV}$, whereas FCA dominates for $h\nu < 2\,\mathrm{eV}$. Coherent TPA, on the other hand, is unlikely for photon energies below half of the bandgap for the direct optical interband transition, i.e. $h\nu < 1.7\,\mathrm{eV}$ ($\lambda > 730\,\mathrm{nm}$). This statement is important because many laser experiments with Si nowadays are performed with Ti:sapphire femtosecond (fs) lasers operating in this wavelength range at high intensity. The above findings were, however, obtained at a low laser pulse repetition rate of 20 Hz only [1] whereas fs lasers typically provide repetition rates of 1 kHz with amplifiers or even 80 MHz in the oscillator mode.

The lifetime of thermalized electrons in the conduction band (CB) of Si, or equivalently, of thermalized electron-hole (eh) pairs ranges around $\tau_{eh} \approx 10\,\mu\mathrm{s}$ for intrinsic and weakly doped Si samples [2–4]. This relatively long lifetime reflects the indirect character of the optical interband transition in Si and is much longer than the typical duration of ultrashort (fs to ps) or even short (ns to µs) laser pulses. Therefore eh pairs can accumulate in Si during long laser pulses and/or during a pulse train of about 100 kHz or higher repetition rate. This leads to increasingly strong absorption of the laser beam by free charge carriers in two ways (i) FCA is possible within the same laser pulse (a) by "hot" charge carriers (directly after generation) and (b) by "cold" carriers in relatively long laser pulses ("cooling" within about 100 fs [6]). (ii) FCA by "cold" carriers occurs in the subsequent laser pulse if its delay is shorter than the eh pair lifetime.

FCA has a long history of more than half a century (cf. e.g. [5]), and was at first investigated by standard spectroscopy and conventional free charge carrier generation. With the advent of lasers, however, the contactless and well confined photo generation of free carriers has become amenable, convenient, and increasingly important in both, laser processing and diagnostics.

In this paper the same Ti:sapphire laser is applied in both operational modes, continuous wave (c.w.) and fs pulse trains, to investigate the nonlinear optical behavior of the same 10 µm thin Si sample by measuring the aver-

Send offprint requests to:
⋆ *Present address:* per-christian.heisel@ipht-jena.de

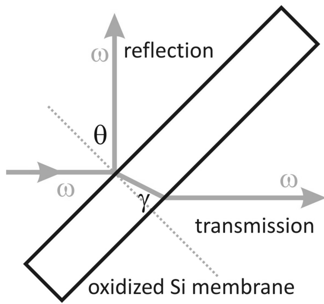

Fig. 1 Scheme of the experiments to compare laser beam reflection from and transmission through thin silicon membranes; external angle of incidence $\theta = 45\,^\circ$; propagation angle within silicon $\gamma \approx 11\,^\circ$.

age laser power reflected from and transmitted through this membrane as a function of the incident laser power (fig. 1). The main experimental findings, independently obtained in two laboratories under slightly different conditions, are essentially identical for c.w. and pulsed operation at 800 nm (1.55 eV). They are discussed in terms of FCA and compared to previous findings in the literature.

2 Experiments

For the transmission measurements two similar experimental setups at two institutes, the IPHT (Leibniz Institute of Photonic Technology) and the LRI (Laser Research Institute) are used. Both setups feature a Ti:sapphire laser beam ($\lambda \approx 800$ nm) to irradiate the Si sample at an external angle of incidence $\theta = 45\,^\circ$ (figure 1). Commercial oscillators (IPHT: Coherent Mira 900F, LRI: Spectra Physics, 3941-M3S, Tsunami) provide average powers up to 1 W at 76 MHz and 80 MHz repetition rate, respectively. The pulse durations of 130 fs (IPHT) and 75 fs (LRI) are determined by APE Pulse Scope autocorrelator (IPHT) or a custom built autocorrelator (LRI). At both research facilities, pulsed and c.w. laser irradiation is applied. The beam polarization (p-polarization) is defined by polarizing beam splitters (PBS) combined with two half-wave plates for power adjustment and polarization control.

At the IPHT the 130 fs pulses are prolonged to about 138 ± 4 fs by the calcite PBS as confirmed by the autocorrelation measurements. The incident laser light is focused onto the sample surface by a combination of $f_1 = -50$ mm and $f_2 = 35$ mm lenses to a focal spot diameter of (13 ± 2) µm. The focal plane position is controlled by a z-scan like measurement. The transmitted light is collimated by a $f_3 = 100$ mm lens. Two identical photomultiplier tubes (PMT, Hamamatsu H10720P-110) with neutral density filters (OD>4) are connected to two identical photon counters (SRS, SR430) for simultaneous signal recording in transmission and reflection directions. Furthermore simple air flushing is optionally applied for sample cooling.

At the LRI, the 75 ± 5 fs laser pulses are prolonged to about 96 fs by the optical components including the PBS. The beam is collimated, focused by two lenses ($f_4 = -50$ mm and $f_5 = 35$ mm) with a focal diameter of (13 ± 2) µm. The transmitted light is collected by a lens with $f_6 = 125$ mm. Power meters are used to measure the transmitted and reflected average powers.

The samples are prepared from commercial $\langle 100 \rangle$-Si wafers by chemical etching using tetramethylammonium hydroxide (TMAH) to produce thin membranes of $3{\times}3\,\mathrm{mm}^2$ area and a thickness of $z_m \approx 10$ µm. The wafers are slightly p-doped ($3 \ldots 6 \cdot 10^{14}\,\mathrm{cm}^{-3}$). Prior to investigations, the membranes are cleaned by using acetone and hydrofluoric acid to remove dirt and old oxide layers, respectively. In contact with air, the clean surfaces oxidize under dark room conditions reaching an equilibrium thickness of (2.5 ± 0.5) nm within 48 hours (cf. e.g. [7]).

3 Results and Discussion

Continuous wave and pulsed laser radiation ($\lambda = 800$ nm) were applied at $45\,^\circ$ external angle of incidence onto thin, naturally oxidized Si membranes of about 10 µm thickness. Figure 2 shows the results of laser beam reflection from (part A) and transmission through the membrane (part B) as a function of the incident average laser power P_{in} up to about 0.8 W on the sample, equivalent to average intensities of up to $4.3 \cdot 10^5\,\mathrm{W/cm}^2$ (IPHT and LRI). It is pointed out that the same transmission values are measured for rising or decreasing laser power P_{in} (i. e. no hysteresis).

Laser beam reflection P_{re} displays a nearly perfect linear dependence on the incident laser power P_{in} (part A, fig. 2). This finding is in agreement with previous reports (cf. e.g. [8]) and confirms the validity of the Fresnel equations using the optical constants of the sample under ambient conditions. The transmitted laser power P_{tr} deviates, however, considerably from linearity (part B, fig. 2) for both, pulsed and c.w. laser irradiation: Starting with an initial linear increase of P_{tr} for low power $P_{in} < 0.3$ W, the transmission reaches a maximum value at $P_{in} \approx 0.5$ W for c.w. and at 0.6 W for pulsed irradiation. For higher laser power P_{in} the transmission signal P_{tr} decreases again. This behavior is slightly affected by air flushing of the sample, yielding higher P_{tr} values (fig. 2, part B). Contributions from internally reflected beams to the transmitted laser power P_{tr} are negligible ($\leq$ about 2%) because of the high reflection losses at the interfaces, even without any account for laser beam attenuation by absorption and/or scattering. The average pulse peak intensities on the sample amount to $41\,\mathrm{GW/cm}^2$ (IPHT) and $59\,\mathrm{GW/cm}^2$ (LRI) averaged over the beam cross section and the pulse duration.

Following the essence of many articles on laser interactions with Si, the discussion at first is focused on

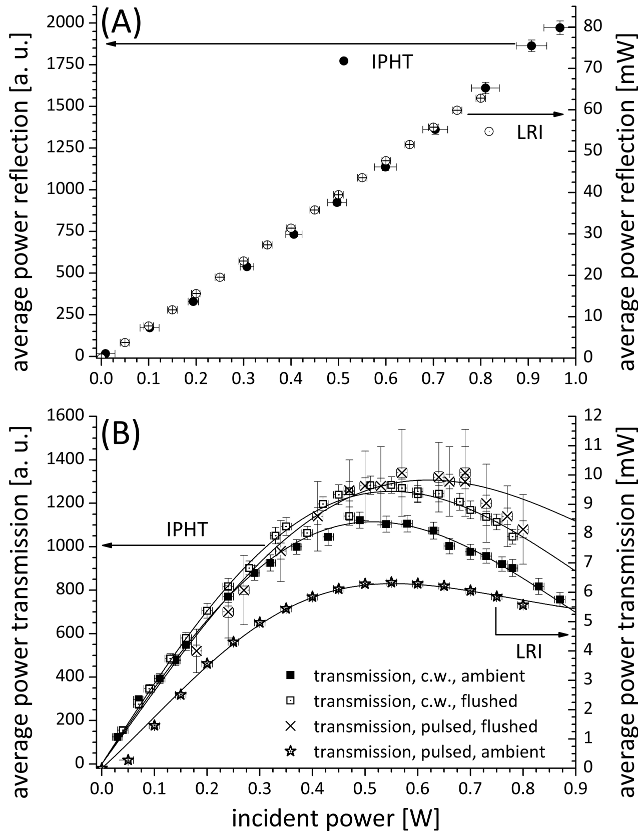

Fig. 2 Average laser power reflected from **(A)** and transmitted through **(B)** a 10 µm thin Si membrane as a function of the incident average laser power measured at IPHT and LRI in c.w. and fs laser pulsed operation at 800 nm with and without air flushing of the sample (cf. text)

FCA as the dominant effect controlling the above experimental findings (cf. e.g. [1,4,6,8–21]). Afterwards possible contributions from e.g. coherent TPA and/or multiphoton excitation will be discussed which, however, can result in a saturation of the laser beam transmission only, but not in its observed decrease with increasing incident power (part B, fig. 2). Furthermore laser induced sample heating will be considered as well to obtain a consistent picture of the new results.

Laser induced FCA has been investigated in many laboratories under very different conditions (cf. e.g. [1,8, 15,18–26]). It typically depends on the sample thickness and irradiation details like the wavelength, c.w. or pulsed laser operation, pulse repetition rate, temporal and spatial pulse shapes. Furthermore, the detection method of the transmitted light is of importance like e.g time or individual pulse resolved detection or pulse train averaged records. As a result, different functionalities between the incident and the transmitted laser light are observed and in many cases prohibit their direct comparison as is easily verified if looking at the many different ways of data presentation in the literature.

Looking at the related literature, such a transmission behavior, i.e. with a maximum in the transmitted power (intensity, fluence) followed by a pronounced decrease, was implicitly reported by Yamada et al. [15] for the irradiation of a 0.6 µm thin Si layer on sapphire by $\tau_p = 250$ ns dye laser pulses at 590 nm: after transformation of their experimental transmission coefficients (Fig. 3 in [15]) to the transmitted intensity I_{tr} (Fig. 3) a maximum of $I_{tr} = 3$ a.u. is observed at the incidence fluence $\Phi_{in} \approx 0.35\,\mathrm{J/cm^2}$ and a steep decrease of I_{tr} towards higher incident fluences. For large Φ_{in} values a constant transmission level of $I_{tr} \approx 1.5$ a.u. is observed (Fig. 3).

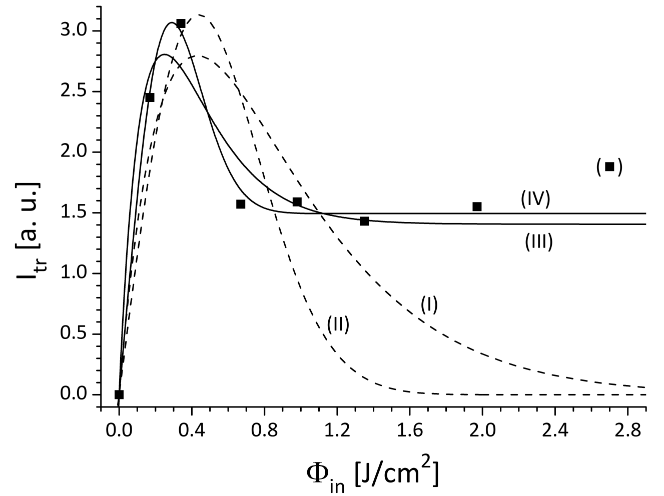

Fig. 3 Experimental transmission values I_{tr} from Yamada et al. [15] as a function of the incident laser pulse fluence Φ_{in} (590 nm, 250 ns) with the value pair ($\Phi_{in} = 0$, $I_{tr} = 0$) added. The fitting curves i to iv are explained in the text.

It is challenging to find suitable fitting curves for the laser transmission data in part B of fig. 2 and in fig. 3 and to rationalize these findings. To begin with, it is assumed that the effective absorption coefficient of the sample $\alpha_{eff} = \alpha_1 + \alpha_{FCA}$ is composed of α_1, the linear, small signal absorption coefficient of unperturbed Si, and the FCA contribution α_{FCA}. Usually the FCA coefficient α_{FCA} is set proportional to the absorption cross section σ_{eh} and the density of eh pairs $n_{eh} = n_e = n_h$ upon photo generation: $\alpha_{FCA} = n_{eh} \cdot \sigma_{eh}$ (cf. e.g. [1,18,20]). The eh pair distribution along the optical pathway in Si is here assumed to be approximately homogeneous because charge carrier diffusion is relatively fast in Si [1] and a stationary n_{eh} value builds up during the measurement time. The measured transmitted laser power then is in both cases, c.w. or pulsed laser operation, related to the homogeneous stationary n_{eh} concentration and therefore a z-independent constant α_{FCA} value. Both depend, however, on I_0 i.e. $n_{eh} = n_{eh}(I_0)$ and $\alpha_{FCA} = \alpha_{FCA}(I_0)$, with I_0 being the intensity directly behind the entrance Si/SiO_2 interface. In addition σ_{eh} depends on n_{eh} [6,10], i. e. $\sigma_{eh} = \sigma_{eh}(n_{eh}(I_0))$. As a result the relation between the intensities $I(z_m)$ directly in front of the exit Si/SiO_2 interface and a given I_0 value

follows the relation

$$I(I_0, z_m) = I_0 \cdot \exp(-\alpha_{eff} z_m) \qquad (1)$$
$$= I_0 \cdot \exp(-\alpha_1 z_m) \cdot \exp(-n_{eh}\sigma_{eh} z_m).$$

The geometric laser path length through the Si membrane z_m is given by $z_m = d_{Si}/\cos\gamma$. For fixed z_m the calculated and measured intensities at $z = z_m$ depend on I_0, n_{eh} and σ_{eh} while z_m, α_1 are constant values. The n_{eh} value is dominated by the optical generation of free carriers, their ambipolar diffusion within and out of the probed volume, and eh pair recombination [1]. The increase of σ_{eh} with n_{eh} is due to increasing carrier-carrier scattering taking place at $n_{eh} > 2 \cdot 10^{17}\,\mathrm{cm}^{-3}$ [6]. As a first approach $\alpha_{FCA} = n_{eh}\sigma_{eh}(n_{eh}) = \kappa_n I_0^n$ is selected with $n = 1$ or 2, implemented into eq. 1 and tested in fig. 3 using the transformed data of Yamada et al. [15] (cf. curves i and ii). Obviously curves i (for $n = 1$) and ii (for $n = 2$) fail to reproduce the steep I_{tr} increase, the position of the I_{tr} maximum and the steep I_{tr} decrease to the plateau of nearly constant I_{tr} values for large Φ_{in} values. This failure is reflected by the small correlation coefficient below 0.5 for curves i and ii. It turns out necessary and sufficient, however, to introduce into eq. 1 a further parameter I_c (cf. eq. 2). For $I_0 \geq I_c$:

$$I(I_0) = (I_0 - I_c)\,F \cdot \exp(-E_n I_0^n) + F I_c$$
$$= I_0 F \cdot \exp(-E_n I_0^n) - I_c F \cdot \exp(-E_n I_0^n) + F I_c$$
$$= I_0 F \cdot \exp(-E_n I_0^n) + I_c F \cdot [1 - \exp(-E_n I_0^n)] \qquad (2)$$

In eq. 2 the abbreviations $F = \exp(-\alpha_1 z_m)$ and $E_n = \kappa_n z_m$ with $n = 1$ or 2 are used. For $I_0 < I_c$ this eq. 2 however gives the physically unreasonable result that $I(I_0) > I_0 \exp(-\alpha_1 z_m)$, i.e. laser beam transmission larger than that expected from one photon absorption. As too little data is available in this small range to determine the behavior accurately we define for $I_0 < I_c$:

$$I(I_0) = I_0 F = I_0 \cdot \exp(-\alpha_1 z_m). \qquad (3)$$

The resultant fit curves iii (for $n = 1$) and iv (for $n = 2$) nicely match the experimental findings as confirmed by their large correlation coefficients of 0.91 and 0.99, respectively. The preferred fit curve iv is based on the parameters $F = 0.74$ for $\alpha_1 = 5000\,\mathrm{cm}^{-1}$ [27,28] and $z_m = 0.6\,\mu\mathrm{m}$ [15], $I_c = 0.14\,\mathrm{J/cm}^2$ together with the scaling factors $I_0/\Phi_{in} = 0.80$ and $I(I_0, z_m)/I_{tr} \approx 0.05\,\mathrm{J/cm}^2$ for the abscissa and ordinate scales in fig. 3, respectively. The I_0/Φ_{in} value describes the laser beam attenuation ($\lambda = 590\,\mathrm{nm}$) by Fresnel reflection at the air/sapphire and sapphire/silicon interfaces upon entering the Si sample [29]. The $I(I_0, z_m)/I_{tr}$ value implies that e.g. the maximum I_{tr} [a.u.] value corresponds to $I(I_0, z_m) \approx 0.15$ $\mathrm{J/cm}^2$, i.e. the laser beam value before leaving the Si sample through the Si/SiO_2 and SiO_2/air interfaces at the rear side [29]. The obtained parameter I_c can be understood as a constant amount of incident laser energy per pulse which contributes to the linear absorption (α_1) but not to FCA. Such a behavior is expected if e.g. part of the generated eh pairs are out of resonance with the incident laser beam.

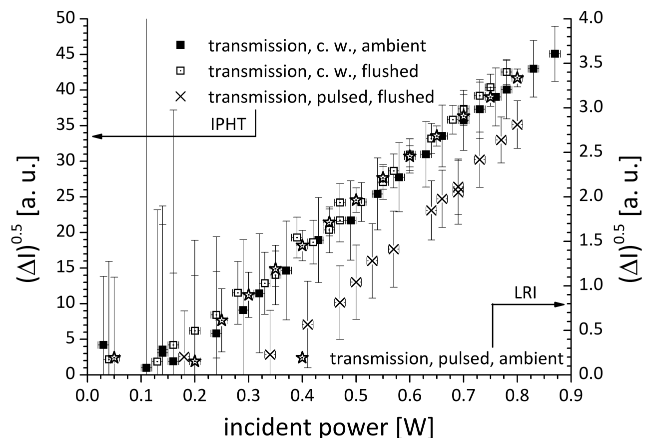

Fig. 4 The square root $(\Delta I)^{0.5}$ of the difference $\Delta I(I_0) = I^0(I_0) - I(I_0) \sim P_{tr}^{calc}(P_{in}) - P_{tr}^{meas}(P_{in})$ representing the FCA contribution as a function of the incident laser power P_{in} (cf. text).

It appears attractive to compare the results by Yamada et al. (Fig. 3) to the data obtained at IPHT and LRI using Ti:sapphire lasers ($\lambda = 800\,\mathrm{nm}$) and $10\,\mu\mathrm{m}$ thick Si membranes (Fig. 2, part B). Common features of both experimental series are their pronounced maxima of the transmitted power (pulse energy fluence) upon increasing the average incident power (fluence). The available and applied Ti:sapphire laser power seems to be insufficient to achieve a constant transmitted power in Fig. 2 B (plateau formation) in analogy to the finding in Fig. 3.

It is instructive to plot the experimental data of fig. 2, part B in a different form by calculating the difference

$$\Delta I(I_0) = I^0(I_0) - I(I_0) \qquad (4)$$

with $I^0(I_0) \equiv I_0 \cdot \exp(-\alpha_1 z_m)$. $\Delta I(I_0)$ describes the FCA related deviation from pure 1-photon absorption and is calculated by subtracting the measured transmitted intensity $I_{tr}(I_0)$ from the value $I^0(I_0)$ calculated using $\alpha_1 = 604\,\mathrm{cm}^{-1}$ [30] and $z_m = 10\,\mu\mathrm{m}$. Plotting $\sqrt{\Delta I(I_0)}$ shows an approximately linear relation between $\sqrt{\Delta I(I_0)}$ and $P_{in} \sim I_0$ in the investigated power range (Fig. 4). For all four data sets the trend line intersects the abscissa at a value $P_{in} > 0$, indicating a threshold for the development of $\Delta I(I_0) \geq 0$ with the P_{in} threshold being related to the I_c term in eq. 2. The small values $\sqrt{\Delta I(I_0)}$ measured below the threshold P_{in} value (Fig. 4) may be due to other contributing mechanisms (cf. below) as zero values are expected when eq. 3 is considered for $I_0 < I_c$. The threshold in this model (I_c in eq. 2) represents a constant part of P_{in} contributing to linear absorption only, but not to FCA (cf. above).

The approximately linear plots $\sqrt{\Delta I\left(I_{0}\right)}$ vs. P_{in} in Fig. 4 confirm that $\alpha_{FCA} \sim I_{0}^{n}$ with $n=2$. Any other value of n results in significant deviations from linearity. The dependence of $\alpha_{FCA}=n_{eh}\sigma_{eh}\left(n_{eh}\right)$ on I_{0}^{2} can be rationalized by using the recent paper of Meitzner et al. [6]: the dependence of σ_{eh} (called σ_{FCA} in [6]) on the free carrier concentration n_{eh} is graphed in Fig. 4 of [6]. Redrawing this graph with linear abscissa scale $n_{eh} \leq 3 \cdot 10^{20}\,\mathrm{cm}^{-3}$ reveals to a first approximation that $\sigma_{eh} \sim n_{eh}$ or $\sigma_{eh}=\sigma_{0}n_{eh}$ with the proportionality constant σ_{0} yielding $\alpha_{FCA}=n_{eh}\sigma_{eh}\left(n_{eh}\right)=\sigma_{0}n_{eh}^{2}$. Assuming furthermore $n_{eh} \sim P_{in}$ or I_{0}, because eh pairs are generated by linear 1-photon absorption, then $n_{eh}=\kappa I_{0}$. This yields $\alpha_{FCA}=\sigma_{0}n_{eh}^{2}=\sigma_{0}\kappa^{2}I_{0}^{2}=\kappa_{2}I_{0}^{2}$ as observed in both our results and those of Yamada et al. [15].

It is pointed out that the FCA contribution is based on two sequential 1-photon absorption processes and essentially different from coherent 2-photon absorption. In FCA the first photon serves to generate an eh pair (interband transition) which in the second step undergoes an 1-photon intraband excitation within the conduction band (electron) or the valence band (hole). The accumulation of an equilibrium density of eh pairs during pulsed or c.w. laser irradiation decouples the rate equations of the first and the second steps in FCA. The absence (or minor influence) of coherent 2- or multiphoton absorption is immediatedly evident from the very similar results obtained with c.w. and fs pulsed laser irradiation (figs. 2 and 4).

The effect of laser induced sample heating can be fairly high as e.g. in case of 0.5 µm thin Si layers on sapphire yielding $\Delta T \leq 900\,\mathrm{K}$ [26] or very small for Si wafers yielding $\Delta T \leq 10\,\mathrm{K}$ [31]. In our intermediate case of 10 µm thin Si wafers, the laser induced temperature rise was observed by an IR camera to be $\Delta T \approx 10\,\mathrm{K}$. Application of the known temperature dependence $\alpha(T, 800\,\mathrm{nm})$ of the Si small signal absorption coefficient [28, 32] shows that this temperature rise reduces the laser beam transmission by about 1 % only (9 % in case of $\Delta T=100\,\mathrm{K}$). Purging of the Si sample with ambient air increased the c.w. laser beam transmission by about 15 % or less (fig. 2). The relation between the FCA contribution $\Delta I(I_{0})$ and the incident laser power P_{in} (slope $d\Delta I(I_{0})^{0.5}/dP_{in}$), on the other hand, remains unaffected (fig. 4).

The correlation between the fit parameters in Fig. 2 B and the measurement values is established by the use of $\alpha_{1}=604\,\mathrm{cm}^{-1}$, $z_{m}=10\,\mu\mathrm{m}$, and $I_{0}=0.845 \cdot P_{in}$ (Fresnel reflection at the air/SiO_2 and Si/SiO_2 interfaces [29]). Values of $0.15\,\mathrm{W} \leq \mathrm{I_c} \leq 0.2\,\mathrm{W}$ are found for the c.w. and $0.24\,\mathrm{W} \leq I_{c} \leq 0.24\,\mathrm{W}$ for the fs laser experiments in agreement with the plots in Fig. 4. Equation (2) and the above relation $\alpha_{FCA}=\sigma_{0}n_{eh}^{2}=\kappa_{2}I_{0}^{2}$ are used to estimate the stationary concentration of free charge carriers by $n_{eh}=I_{0} \cdot \sqrt{E_{2}/\left(\sigma_{0}z_{m}\right)}$. The unknown value σ_{0} is derived from ref. [20], for $\lambda=800\,\mathrm{nm}$ (IPHT & LRI) and $\lambda=590\,\mathrm{nm}$ (Yamada et al. [15]) in different ways. For $\lambda=800\,\mathrm{nm}$ the value $\sigma_{eh}=\sigma_{0}n_{eh} \approx 10^{17}\,\mathrm{cm}^{2}$ with $n_{eh}=1.4 \cdot 10^{18}\,\mathrm{cm}^{-3}$ is derived from Figs. 2(c), 3(a) and 3(b) of ref. [20]. This value σ_{eh} is roughly estimated to lie between the σ_{eh} values of nanocrystalline and bulk Si and leads to $\sigma_{0}\,(800\,\mathrm{nm}) \approx 5 \cdot 10^{-36}\,\mathrm{cm}^{5}$ resulting in $1.7 \cdot 10^{18}\,\mathrm{cm}^{-3} \leq n_{eh}\left(I_{0}=0.1\,\mathrm{W}\right) \leq 2.1 \cdot 10^{18}\,\mathrm{cm}^{-3}$ and $1.5 \cdot 10^{19}\,\mathrm{cm}^{-3} \leq n_{eh}\left(I_{0}=0.9\,\mathrm{W}\right) \leq 2.0 \cdot 10^{19}\,\mathrm{cm}^{-3}$. These values are placed well below the Si damage threshold.

The value $\sigma_{0}\,(\lambda=590\,\mathrm{nm}) \approx 1.2 \cdot 10^{-39}\,\mathrm{cm}^{5}$, on the other hand, is extrapolated using the relation $\sigma_{FCA}(\lambda)=(5 \pm 2) \cdot 10^{-9}\lambda^{2.0 \pm 0.3}\,\mathrm{cm}^{2}$ [20] ($\sigma_{FCA}(\lambda)$ corresponds to $\sigma_{eh}(\lambda)$ in this paper). Using this value $\sigma_{0}=(\lambda=590\,\mathrm{nm})$, eh pair concentrations $7 \cdot 10^{20}\,\mathrm{cm}^{-3} \leq n_{eh} \leq 2 \cdot 10^{22}\,\mathrm{cm}^{-3}$ at $I_{0}=0.1\,\mathrm{Jcm}^{-2}$ and $2.5\,\mathrm{Jcm}^{-2}$ is in agreement with the reported laser damage of the sample.

To conclude, the applied approximations and fit procedures appear applicable. The fit curves in Fig. 2, part B and Fig. 3 were obtained using eq. 2 and $n=2$. In case of the LRI data a small abscissa scale offset of 0.025 W turned out helpful. Overall the obtained results can be fitted and rationalized within a simple model of FCA. This finding is encouraging particularly as both laser wavelengths might generate a complex situation: FCA at these wavelength can compete with the indirect optical transition of Si, i. e. the generation of eh pairs. The empirically found power law (or pulse energy fluence) can be rationalized by a linear dependence of the eh pair absorption cross section $\sigma_{eh}=\sigma_{0}n_{eh}$ on the density of eh pairs in the investigated n_{eh} region and by assuming a linear relation between the incident laser power and the stationary concentration n_{eh} of free carriers. Thus a simple and consistent picture has been established. We expect an $I(I_{0})$ plateau – like that in Fig. 3 – corresponding to $(40 \pm 10)\%$ of the maximum $I(I_{0})$ values in part B of Fig. 2 in the so far experimentally non-accessible region $P_{in}>1\,\mathrm{W}$.

4 Summary and Conclusion

Summarizing, the above results appear to pave the way for further well designed experimental and theoretical investigations of the complex interactions between Ti:sapphire lasers and thin crystalline silicon samples. This combination of a technologically relevant and flexible laser system and a prominent semiconductor appears very promising in particular for sample thicknesses $z_{m} \approx l_{abs}(\lambda_{L})$ lying in the range of the relevant absorption length $l_{abs}(\lambda_{L})$.

The absorption of Ti:sapphire laser light by slightly p-doped silicon was investigated under c.w. and fs pulsed laser operation using a 10 µm thin membrane. The average laser power incident onto the sample was increased up to about 1 W. This variation revealed a strong nonlinear power (intensity) dependence of the beam transmission through the sample whereas laser beam reflec-

tion remained a linear function. The nonlinearity observed with the laser beam transmission is essentially the same for c.w. and pulsed laser irradiation and mainly attributed to free carrier absorption (FCA) in silicon. Laser induced sample heating and coherent two- and/or multi-photon absorption were shown to be of minor importance only.

Similar results previously obtained by using a pulsed dye laser at 590 nm irradiating a 0.6 µm thick Si layer on sapphire [15] show a pronounced maximum followed by a lower constant transmission for further increasing input intensity (Fig. 3). This complex transmission behavior could nicely be fitted by a simple FCA model.

The FCA model has been applied to the only laser transmission measurements, which to our knowledge display the pronounced maximum in the transmitted laser power (energy fluence) as a function of the laser input power (energy fluence). This maximum is possibly due to the fact that both excitation wavelengths are in resonance with the indirect optical transition of Si. Most of the published FCA articles on Si refer to longer wavelengths.

The applied FCA model is based on several assumptions:

- constant Fresnel reflection factors for the laser beams at the Si membrane interfaces (e.g. no intensity dependence),
- a laterally and axially homogeneous distribution of eh pairs in the laser irradiated and probed volume (e.g. independent on the local laser beam intensity), thus decoupling the two absorption processes of this FCA model,
- two optically linear absorption processes, i.e. for eh pair generation and their excitation with negligible coherent 2- or multi-photon absorption,
- an effective absorption coefficient $\alpha_{eff} = \alpha_1 + \alpha_{FCA}$ (e.g. independent on the Si sample temperature),
- a constant linear absorption coefficient α_1 (Beer's law),
- an empirical ansatz for the absorption coefficient $\alpha_{FCA} = n_{eh}\sigma_{eh}$ for FCA with e.g. σ_{eh} being independent on the eh pair temperature (cf. e.g. [3]), but dependent on the eh pair density (cf. e.g. [10]), and
- negligible FCA in the $0 \leq I_0 \leq I_c$ region with I_c being a critical minimum value up to which laser excitation possibly does generate eh pairs but no FCA.

As a result, fitting the experimental data withe the above FCA model revealed a power law $n \approx 2$ of $\alpha_{FCA} = \kappa_n \cdot I^n$, which is confirmed by the linear plots in Fig. 4. A physical interpretation of $n \approx 2$ is given by assuming that the stationary density e_{eh} of free charge carriers is proportional to the incident laser intensity I_0 and that the absorption cross section $\sigma_{eh} = \sigma_0 n_{eh}$ is proportional to n_{eh} [6] yielding the FCA absorption coefficient $\alpha_{FCA} = \kappa_2 I_0^2$. However, there is a need for further experimental data to test the FCA model in more detail.

Acknowledgements

Institutional funding by the Thuringian Ministry of Education, Science and Culture (TMBWK) is gratefully acknowledged as well as support from the CSIR NLC rental pool and the National Research Foundation of South Africa. The authors thank Dr. E. Kessler for the preparation of the silicon membranes, Dr. J. Plentz for his conductivity measurement to determine the dopant concentration, Dr. F. Falk for fruitful discussions and BSc K. Ritter for several transmission measurements at Jena. W. Ndebeka acknowledges the support from the African Laser Center.

References

1. J. M. Moison, F. Barthe, M. Bensoussan, Phys. Rev. B **27,** (1983) 3611
2. J. Dziewior, W. Schmid, Appl. Phys. Lett. **31,** (1977) 346
3. D. J. Sandiford, Proc. Phys. Soc. **71,** (1958) 1002
4. C. M. Horwitz, R. M. Swanson, Solid-State Electron. **23,** (1980) 1191
5. H. B. Briggs, R. C. Fletcher, Phys. Rev. **91,** (1953) 1342
6. J. Meitzner, F. G. Moore, B. M. Tillotson, S. D. Kevan, G. L. Richmond, Appl. Phys. Lett. **103,** (2013) 092101
7. C. Logofatu, C. C. Negrila, R. V. Ghita, F. Ungureanu, C. Cotirlan, C. G. A. S. Manea, M. F. Lazarescu, *Study of SiO_2/Si Interface by Surface Techniques* (www.intechopen.com) (2011) 23-42
8. K. Sokolowski-Tinten, J. Bialkowski, D. von der Linde, Phys. Rev. B **51,** (1995) 14186
9. V. Grivitskas, M. Willander, J. Vaitkus, Solid-State Electron. **27,** (1984) 565
10. B. E. Sernelius, Phys. Rev. B **39,** (1989) 10825
11. H. Y. Fan, W. Spitzer, R. J. Collins, Phys. Rev. **101,** (1956) 566
12. W. Spitzer, H. Y. Fan, Phys. Rev. **108,** (1957) 268
13. D. K. Schroder, R. N. Thomas, J. C. Swartz, IEEE T. Electron Dev. **ED-25** (1978) 254
14. K. G. Svantesson, J. Phys. D: Appl. Phys. **12,** (1979) 425
15. M. Yamada, H. Kotani, K. Yamamoto, K. Abe, Phys. Lett. **85A,** (1981) 191
16. R. A. Soref, B. R. Bennett, IEEE J. Quantum Elect. **QE-23,** (1987) 123
17. D. K. Schroder, IEEE T. Electron Dev. **ED-44,** (1997) 160
18. J. Linnros, J. Appl. Phys. **84,** (1998) 275
19. J. Linnros, J. Appl. Phys. **84,** (1998) 284
20. R. D. Kekatpure, M. L. Brongersma, Nano Lett. **8,** (2008) 3787
21. M. De Laurentis, A. Irace, J. Solid State Phys. **2014,** (2014) 291469
22. J. E. Geusic, S. Singh, D. W. Tipping, T. C. Rich, Phys. Rev. Lett. **19,** (1967) 1126
23. J. M. Ralston, R. K. Chang, Appl. Phys. Lett. **15,** (1969) 164
24. W. B. Gauster, J. C. Bushell, J. Appl. Phys. **41,** (1970) 3850
25. J. F. Reintjes, J. C. McGroddy, Phys. Rev. Lett. **30,** (1973) 901

26. J. M. Liu, H. Kurz, N. Bloembergen, Appl. Phys. Lett. **41,** (1982) 643
27. E. D. Palik, G. Ghosh, *Handbook of Optical Constants of Solids* (Academic Press, San Diego 1998)
28. G. E. Jellison, F. A. Modine, Appl. Phys. Lett. **41,** (1982) 180
29. Fresnel reflection calculated by using $n(\text{air}) = 1.00$, $n(\text{sapphire}) = 1.77$, $n(\text{Si}) = 3.97$ and $n(\text{SiO}_2) = 1.46$ for 590 nm or $n(\text{air}) = 1.00$, $n(\text{Si}) = 3.75$, and $n(\text{SiO}_2) = 1.45$ for 800 nm [27]
30. G. P. Nyamuda, E. G. Rohwer, C. M. Steenkamp, H. Stafast, Appl. Phys. B **104,** (2011) 735
31. J. R. Goldmann, J. A. Prybyla, Phys. Rev. Lett. **72,** (1994) 1364
32. B. K. Sun, X. Zhang, C. P. Grigoropoulos, Int. J. Heat Mass Transfer **40,** (1997) 1591